Personalized Heart Digital Twins Detect Substrate Abnormalities in Scar-dependent Ventricular Tachycardia

Authors:

1. Michael C Waight; MBBS, BSc(Hons), MRCP [a, b]
2. Adityo Prakosa; PhD [b]
3. Anthony C Li; MD(Res), MBBS, BSc(Hons), MRCP [a,c]
4. Nick Bunce; MD, MBBS, BSc, MRCP [c]
5. Anna Marciniak; MBBS, PhD, MRCP [c]
6. Natalia A Trayanova; PhD, FHRS, FAHA [b *]
7. Magdi M Saba; MD, MSc, FHRS [a,c,d *]

* NT and MS are joint senior co-authors.

Authors' affiliations:

a) City St George's, University of London

Cranmer Terrace

London, SW17 0RE

United Kingdom

b) Alliance for Cardiovascular Diagnostic and Treatment Innovation

Johns Hopkins University

3400 N. Charles Street

Baltimore MD 21218

c) St George's University Hospitals NHS Foundation Trust

Blackshaw Road

London, SW17 0QT

United Kingdom

d) Cleveland Clininc London

33 Grosvenor Pl

London, SW1X 7HY

United Kingdom

Running title: Digital Twins Detect Substrate Abnormalities in VT

Corresponding author:

Dr Michael Waight

City St George's, University of London

Cranmer terrace, London, SW17 0RE

Email: michaelwaight@nhs.net

Word Count: 5308

Abstract

Background

Current outcomes from catheter ablation for scar-dependent ventricular tachycardia (VT) are limited by high recurrence rates and long procedure durations. Personalized heart digital twin technology presents a non-invasive method of predicting critical substrate in VT, and its integration into clinical VT ablation offers a promising solution. The accuracy of digital twins' predictions to detect invasive substrate abnormalities is unknown. We present the first prospective analysis of digital twin technology in predicting critical substrate abnormalities in VT.

Methods

Heart digital twin models were created from 18 patients with scar-dependent VT undergoing catheter ablation. Contrast-enhanced cardiac magnetic resonance images were used to reconstruct finite element meshes, onto which regional electrophysiological properties were applied. Rapid-pacing protocols were used to induce VTs and define the VT circuits. Predicted optimum ablation sites to terminate all VTs in the models were identified. Invasive substrate mapping was performed, and the digital twins merged with the electroanatomical map. Electrogram abnormalities and regions of conduction slowing were compared between digital twin-predicted sites and non-predicted areas.

Results

Electrogram abnormalities were significantly more frequent in digital twin-predicted sites compared to non-predicted sites (468/1029 [45.5%] versus 519/1611 [32.2%], $p < 0.001$). Electrogram duration was longer at predicted sites compared to non-predicted sites (82.0ms [± 25.9ms] versus 69.7ms [± 22.3ms], $p < 0.001$). Digital twins correctly identified 21/26 (80.8%) of deceleration zones seen on isochronal late activation mapping.

Conclusions

Digital twin predicted sites display a higher prevalence of abnormal and prolonged electrograms compared to non-predicted sites, as well as accurately identifying regions of conduction slowing. Digital twin technology may help improve substrate-based VT ablation.

Clinical Trial Registration

Clinical Trial Registration Number: NCT04632394

URL: https://clinicaltrials.gov/study/NCT04632394?cond=NCT04632394&rank=1

Key Words

Ventricular tachycardia

Digital twin

Catheter ablation

Cardiac MRI

Electroanatomical mapping

Clinical Perspective

What is new?

- MRI-based heart digital twins were created from patients with scar-dependent VT to assess their accuracy in detecting critical substrate abnormalities during VT ablation.
- The invasive electrophysiological properties of sites predicted to be of importance in sustaining VT by heart digital twins have never previously been studied.
- The personalized heart digital twins accurately detected both substrate and functional abnormalities during invasive VT ablation.

What are the clinical implications?

- Digital twin technology may improve the efficacy and act as a guide for catheter ablation of ventricular tachycardia.
- Utilising digital twins in VT ablation may help reduce procedure time, complications and length of hospital stay in the future.

Key Question

Can personalized heart digital twin technology be used to detect substrate abnormalities in patients with scar-dependent ventricular tachycardia (VT) undergoing catheter ablation?

Key Finding

Areas predicted by heart digital twins to be of critical importance in the formation of VT display a significantly greater proportion of substrate and functional abnormalities compared to non-predicted sites.

Take-home Message

Heart digital twins accurately detect substrate abnormalities in those with scar-dependent VT. This technology may improve the efficacy and act as a guide for catheter ablation of ventricular tachycardia.

Abbreviations

Abbreviations	
DZ	Deceleration zone
EAM	Electroanatomic map
EGM	Electrogram
ICD	Implantable cardioverter-defibrillator
ICM	Ischemic cardiomyopathy
ILAM	Isochronal late activation mapping
LGE-CMR	Late gadolinium-enhanced cardiac magnetic resonance imaging
LAVA	Local abnormal ventricular activity
LV	Left ventricular
NICM	Non-ischemic cardiomyopathy
PES	Programmed electrical stimulation
RV	Right ventricular
VT	Ventricular tachycardia

Keywords

Ventricular tachycardia

Digital twins

Catheter ablation

Substrate mapping

Electrograms

Introduction

Catheter ablation for scar-dependent ventricular tachycardia (VT) is an established treatment which has been proven to reduce defibrillator shocks and prevent recurrence of arrhythmia in randomised-controlled trials.[1–3] During ablation, the optimum outcome is to induce and map the clinical VT to prove the location of the critical isthmus and confirm its non-inducibility following ablation.[4,5] However, sustained VT is frequently not haemodynamically tolerated, necessitating an alternative ablation strategy, known as substrate ablation, which is principally targeted towards the elimination of abnormal electrograms seen in and around the area of myocardial scar. Techniques include abolition of late potentials[6], local abnormal ventricular activity[7] and scar homogenisation.[8] Despite evidence that VT ablation can effectively treat VT[9], long-term recurrence rates in recent large trials are between 31% and 48%.[10–12] Procedure-related complications are frequent[13] and ablations can last several hours.[14] Therefore, there is a requirement to make VT ablation safer, faster and more effective.

A digital twin is a virtual representation of a system that mimics the structure and function of the system and has a predictive capability, informing decisions that realize value.[15] Medical digital twins, which are computational models of organs (and even patients) created with patient data, have been making significant inroads in medicine to support clinical decision-making.[16] Heart digital twins, which are personalized mechanistic computational models of patient hearts constructed from patient data and representing the functioning of the patient heart, have been used for a number of clinical applications in recent years.[17] They have demonstrated accurate prediction of risk of sudden cardiac death in both ischemic and non-ischemic populations[18–21] by evaluating the arrhythmogenic propensity of the disease-remodelled (fibrotic or scarred) myocardial milieu. Heart digital twins incorporating genetic predisposition[19] or penetrating adiposity[22,23] have recently been used to predict the locations of VT circuits. Heart digital twins have been proposed as the technology that could predict non-invasively, pre-procedure, the optimal personalized targets in patients undergoing VT ablation[24], directly guiding the delivery of lesions that fully eliminate the likelihood of arrhythmia occurrence.

Should this technology become clinical reality, it would potentially improve procedural success, reduce the risk of long-term arrhythmia recurrence and allow for a shorter, more targeted, ablation procedure and therefore reduce complications and length of hospital stay. However, to achieve the full potential of digital twins in improving VT ablation, the technology needs to be evaluated intra-procedurally in the cardiac electrophysiology lab, and its agreement with invasive recordings of patient's electrophysiological activity demonstrated. The invasive electrophysiological characteristics of these digital twin-predicted arrhythmogenic sites has never previously been studied.

We present the first combined prospective clinical and heart digital twin study with the aim of invasively evaluating the accuracy of the personalized model predictions. Specifically, we construct heart digital twins in a cohort of ischemic (ICM) and non-ischemic cardiomyopathy (NICM) patients undergoing ablation for scar-dependent VT and predict the substrate locations most likely to sustain re-entrant arrhythmias. We examine digital twin arrhythmogenesis arising both in the native substrate as well as in the post-ablation substrate – an approach that is unique to our personalized prediction of VT ablation targets. During clinical VT ablation, we perform comprehensive substrate mapping and evaluate electrogram properties at sites deemed of critical importance by the digital twin in order to establish their relation to the conventional substrate-mapping approach to VT ablation. Ascertaining the capabilities of the heart digital twins to predict optimal targets for scar-related VT would open the door to novel means of delivering treatment to patients with VT, and thus chart a pathway for the personalized management of ventricular arrhythmia.

Methods

Data availability

Mesh geometries and simulation data are available upon reasonable request to NT. Patient data used in this study cannot be made publicly available without further consent and ethical approval, owing to privacy concerns. MRI images can be provided by the authors pending St George's Hospital Medical Imaging Department approval and a completed material transfer agreement. Codes for image processing and simulations are available upon reasonable request to the corresponding author.

Study overview

This was a single center prospective study with two phases. Firstly, consecutive patients with scar-dependent VT requiring catheter ablation prospectively underwent late-gadolinium enhanced cardiac MRI (LGE-CMR). From each image, we generated a heart digital twin reflecting the distribution of the patient's scar. Next, arrhythmia inducibility following pacing was tested in the digital twin to determine the optimum ablation sites to terminate all possible VTs in the model. Subsequently, the patient underwent invasive VT ablation that included comprehensive substrate mapping. During VT ablation, the digital twin and the clinical electroanatomical map (EAM) were merged. Electrogram abnormalities were compared between sites predicted by the heart digital twin to be of importance and non-predicted sites and the correspondence evaluated. Figure 1 presents an overview of the study.

Patient population

Consecutive patients with scar-dependent VT in the setting of both ICM and NICM requiring catheter ablation were prospectively recruited. Indications for catheter ablation included recurrent VT or ICD therapy, prohibitive side effects or unwillingness to take anti-arrhythmic drugs. All patients described in this study provided written, informed consent. The study was approved by Health Research Authority (HRA) London – Surrey Research Ethics Committee (21/LO/0083).

Cardiac MRI protocol

Patients underwent pre-procedure LGE-CMR, including a 3D LGE sequence. Details of image acquisition are provided in the supplemental methods. Briefly, LGE-CMR was performed using a 3T Philips Achieva for patients without implantable cardiac devices and a 1.5T Siemens Magnetom Aera (with wideband sequences) for those with devices. LGE-CMR images were acquired using a free-breathing respiratory-navigated sequence with an image resolution of 1.3 x 1.3 x 1.8mm. Only patients with sufficient MRI quality were included, defined as having the entire LV myocardium visible within the MRI field of view, with clearly identifiable scar boundaries and the absence of artifact affecting the scar region.

Generation of the heart digital twin

Acquired 3D LGE-CMR images were used as the basis for the generation of a heart digital twin (a personalized mechanistic computational model) for each patient that represented the electrical functioning of the patient's heart. The digital twin was used to induce VTs and define their circuits, and to derive optimum ablation lesion sets which terminate all VTs a patient's digital twin can sustain. This methodology has been described in detail in previous publications from our group and is outlined in the supplemental methods.[22,24–26]

Construction of a patient's heart geometric model

Endocardial and epicardial boundaries from the 3D LGE-CMR images are contoured and the myocardium categorised as dense scar, borderzone or healthy tissue using a validated full-width half-maximum approach.[27] Finite-element meshes with an average resolution of 400μm were generated, containing approximately 4 million individual nodes.[28] Fibre direction was subsequently applied to the mesh.[29]

Application of electrophysiological properties to the model

Electrophysiological properties were applied to each of the three tissue regions in the patient's heart digital twin. Dense scar was modelled as an electrically inert. Healthy tissue was assigned ventricular

action potential kinetics using the Ten Tusscher ionic model[30]. Borderzone was assigned modified kinetics, characterised by a slower action potential upstroke velocity, reduced peak amplitude, longer action potential duration and reduced cell-cell conductivity.[20] Wavefront propagation was simulated by solving the reaction-diffusion partial differential equation using the opensource software openCARP (https://opencarp.org) on a parallel computing system.[31]

Simulated pacing and ablation protocol

To test VT inducibility in the digital twin, simulated pacing was applied from 7 LV sites, based on a condensed 17-segment AHA model, preferentially delivered to sites of borderzone in order to maximise the likelihood of inducing re-entry. Pacing was delivered as a train of 6 beats at a cycle length of 600ms (S1), followed by up to four premature extrastimuli until VT was observed.[20,23,24]

Ablation in heart digital twins

Application of simulated ablation lesions at primary sites

Once re-entry was identified in the digital twin, each VT was analysed for critical sites including the entrance, isthmus and exit. Simulated ablation lesions were applied to the VT isthmus to terminate re-entry in that location. Simulated ablation lesions have a radius of 3.5mm and are assumed to be transmural. Where feasible, ablation lesions were extended from the isthmus to connect to adjacent regions of non-conducting, transmural dense scar, or anatomical barriers. This was done to avoid the emergence of secondary, iatrogenic VTs following ablation. These lesion sets were subsequently modelled as insulators. Lesions applied to the original substrate during this first round of simulation were labelled “primary sites”.

Repeat simulation and secondary site identification

Following application of primary site ablation lesions, the VT induction and ablation protocol was repeated to assess VT inducibility in the in the post-ablation substrate, consisting of the residual native scar and ablation lesions. If new VTs emerged, further ablation lesion sets were applied in a similar fashion to the primary sites and were termed “secondary sites”. The process was repeated until the

patient's digital twin was no longer inducible to VT. This represents the hallmark of our digital twin approach, and is designed to prevent the emergence of new VTs after the index ablation procedure, thus decreasing redo procedures and re-hospitalization.

Each predicted ablation lesion set typically terminated one VT, but may be extended to also terminate a second VT circuit located in close proximity to the first. "Predicted sites" in our subsequent analysis were considered to be the primary and secondary ablation lesion sites which terminated all VTs during the simulation. Sites of lesion extension to nearby non-conducting barriers to prevent iatrogenic VT were excluded for EGM analysis.

Invasive VT mapping and ablation protocol

Following generation of the heart digital twin, patients underwent clinical VT ablation. Anti-arrhythmic medications were discontinued five half-lives prior to ablation, with the exception of amiodarone which was discontinued one week prior to ablation. Ablation was performed under general anaesthesia. Epicardial access was gained at the operator's discretion as determined by aetiology, presence of epicardial scar on CMR and in those presenting for redo ablation. Where possible, dual left ventricular (LV) access was gained via both the trans-septal and retrograde aortic approaches. Electroanatomical mapping was performed using the Ensite Precision or Ensite X systems and the multipolar Advisor HD Grid mapping catheter (Abbott Laboratories, Chicago, IL, USA). Substrate mapping was performed during right ventricular (RV) pacing at 600ms for three beats followed by an extrastimulus (S2) at 20ms above ventricular effective refractory period. Standard low voltage bipolar thresholds (0.5-1.5mV endocardial, 0.5mV-1.0mV epicardial) were applied.

Following substrate mapping, VT was induced using programmed electrical stimulation (PES) and (if tolerated) mapped using activation and entrainment mapping to identify the critical isthmus and guide ablation. If the VT was not haemodynamically tolerated, a substrate-based approach to ablation was utilised. The procedural endpoint was defined as non-inducibility of all significant VTs following repeat PES.

Integration of the Digital Twin with the Electroanatomical Map

Fiducial landmarks including the left and right coronary cusps and the LV outflow tract from the digital twin were aligned with their counterparts on the EAM once the full invasive geometry and substrate map had been created. Rigid merging of the two maps (digital twin and EAM) was performed using the Ensite Fusion Registration Module. Coregistration was performed by an expert independent of subsequent analysis and blinded to predicted site location. Care was taken to achieve the closest merge possible in all three orthogonal planes. Operators were blinded to the location of the predicted sites or any of the digital twin surfaces at all times. The operators did have access to the conventional LGE-CMR images pre-procedurally in line with current gold standard of care for VT ablation, to help guide the appropriate access routes.

Electrogram analysis

Acquired electrograms were analysed on the Ensite mapping system and using a bespoke MATLAB Runtime. Measurements of electrogram timing and morphological abnormalities were assessed, blinded to location on the EAM and in accordance with accepted literature.[7,32,33] Parameters assessed include bipolar and unipolar voltage, QRS onset, offset and duration, EGM onset, offset and duration and EGM morphological abnormalities. Full description of these abnormalities is outlined in Table S1. Figure S1 shows examples of these measurements and abnormalities.

Comparison of LV endocardial electrograms was made between predicted and non-predicted sites at different tissue regions, based on accepted voltage cut-offs; including dense scar (bipolar amplitude <0.5mV), borderzone (0.5 – 1.5mV) and healthy tissue (> 1.5mV). Electrogram characteristics at primary predicted sites (predicted by the digital twin to be responsible for VTs which arise in the native scar substrate) were compared to secondary sites (those predicted to arise *de novo* following ablation of the primary sites).

Endocardial scar size analysis

Comparison was made between the size of the low voltage region on the EAM and the MRI-defined scar. Total endocardial bipolar and unipolar low voltage area was calculated by contouring the area of low voltage according to accepted criteria (<1.5mV bipolar, < 8.3mV unipolar) and compared with area of MRI-defined scar.

Functional substrate mapping analysis

EGMs from extrastimulus pacing maps were analysed and electrogram abnormalities compared between predicted non-predicted sites. The increase in its duration in response to extrastimulus pacing was compared between predicted and non-predicted regions. During RV pacing, isochronal late activation maps (ILAM) were created using a methodology previously described.[34,35] Briefly, each electrogram was annotated to the last deflection. The total left ventricular activation window was divided into eight colours (isochrones), each representing one eighth of the total LV activation time. A deceleration zone (DZ) was defined as displaying > 3 isochrones within a 1cm radius. Spatial correlation of DZ with predicted areas was analysed. A DZ within 5mm of a predicted area, measured as geodesic distance, was considered spatially related to a predicted site. Analysis was performed for both primary and secondary digital-twin predicted sites.

Statistical analysis

Continuous, normally distributed data are expressed as mean ± standard deviation. Non-parametric data are expressed as median ± interquartile range. Categorical data are expressed as total number and percentage. Linear mixed models were constructed to compare EGM abnormalities between predicted and non-predicted sites, using patients as a random effect. Comparison of continuous, non-parametric data within individuals was done with Mann-Whitney U test. Categorical variables within individuals compared using chi-square tests. Receiver operator curves were used to determine the

optimum voltage cut-offs which correspond to MRI-defined scar. A p value of < 0.05 was taken to indicate statistical significance. Statistical analysis was carried out with SPSS version 30 (IBM Corp, Armonk, NY, USA).

Results

Patient demographics

37 patients with scar-dependent VT were screened of whom 18 had sufficient quality LGE-CMR images for heart digital twin creation. 17/18 (94.4%) were male. Baseline LVEF was 42.3% (± 16.5%). Those with NICM exhibited a higher baseline EF (46.3 ± 10.0% vs 41.5 ± 17.7%) compared to those with ICM. 17/18 (94.4%) were taking beta blockers, 7/18 (38.9%) were taking amiodarone and 3/18 (16.7%) were taking mexiletine. All but one patient had either an ICD or CRT-D *in situ.* Epicardial mapping was performed in 5/18 (27.8%) of cases. Table 1 shows the full baseline demographics of the cohort.

Scar and predicted site distribution and comparison of invasive vs MRI-defined scar size.

Analysis of the distribution of the LGE area from the 3D CMR suggested a preponderance of inferior and lateral scars. Scar location was inferolateral in 5/18 (27.8%) cases, lateral in 4/18 (22.2%) cases, septal in 4/18 (22.2%) cases, inferior in 3/18 (16.7%) cases and anterior in 2/18 (11.1%). During digital twin simulation, a total of 92 predicted sites were identified, including 62 primary and 30 secondary sites. All predicted sites were located within MRI scar. 65/92 (70.7%) were located primarily within borderzone and 27/92 (29.3%) were primarily within dense scar. Average predicted site length and width were 45.5mm (± 40.3mm) and 8.08mm (± 2.31mm) respectively. As shown in Figure 2A, there were no significant differences in the distribution of scar compared to predicted sites, confirming a correlation between scar location and the sites of the VT isthmus observable in the digital twins.

Following co-registration of the digital twins with the EAMs, mean distance between the two surfaces was measured at 3.95mm (± 0.93mm). Table S2 shows the distance for each case between the EAM and the MRI. We next compared the area of low voltage on the electroanatomical map according to accepted cut-offs with the CMR LGE scar. On the EAM, median bipolar low voltage (<1.5mV) area was 28.9 (21.8 – 41.3) cm^2. Unipolar low voltage (<8.3mV) area was 48.4 (32.8 – 59.2) cm^2. On CMR, LGE

scar area was 46.1 (40.4 – 59.2) cm^2. Unipolar low voltage area and MRI scar area were significantly larger than bipolar low voltage area (p = 0.01 and p = 0.02 respectively), however MRI scar area was not significantly different from unipolar scar area (p = 0.89), as shown in Figure 2B. Data on the discrepancy in scar size between EAM and MRI for each patient is available in Table S3. The data suggests a better correspondence between unipolar voltage mapping and the CMR determined scar. Figure S2 shows an example of how the bipolar low voltage area underestimated the scar size relative to the MRI, whereas the unipolar low voltage area appeared more closely aligned. ROC curve analysis revealed an optimum for bipolar voltage in the detection of MRI LGE of 2.3mV (AUC 0.79 [0.78 – 0.79]), which is considerably higher than the traditional 1.5mV threshold typically used.[36] Unipolar voltage ROC curve analysis revealed an optimum cut-off of 7.9mV (AUC 0.78 [0.77 – 0.78]), which is more closely aligned to the accepted value of 8.3mV.[37] ROC curves for this comparison are shown in Figure S3.

Comparison of electrogram abnormalities between predicted and non-predicted sites within scar

Next, we compared electrogram abnormalities between sites on the EAM which correspond to the predictions from the heart digital twin with non-predicted sites. The median total number of EAM points per patient was 1512 (1287 – 2209). A total of 23,794 bipolar, endocardial LV electrograms were analysed of which 7699 were of low voltage (<1.5mV bipolar amplitude) and 2640 points from within dense scar (<0.5mV bipolar amplitude). Within dense scar, there was no difference in bipolar voltage between the predicted and non-predicted sites (0.31mV $\pm$ 0.11mV vs 0.32 $\pm$ 0.11mV, p = 0.69), suggesting that any differences between predicted and non-predicted sites were not simply due to a greater extent of scar in these areas. All electrogram abnormalities were more frequently seen in predicted areas compared to non-predicted areas with the exception of double potentials. Overall, electrogram abnormalities were seen in 468/1029 (45.5%) of predicted sites vs 519/1611 (32.2%) of

non-predicted sites ($p < 0.001$). Measures of electrogram timing differed significantly between predicted and non-predicted sites, with predicted site EGMs displaying longer total duration at 82.0ms (± 25.9ms) compared to 69.7ms (± 22.3ms) at non-predicted sites ($p < 0.001$). Sensitivity and specificity for detection of EGM abnormalities within dense scar was 45.8% (± 23.6%) and 71.1% (± 24.6%) respectively. Crucially, these results demonstrate the unusually high prevalence of electrogram abnormalities at digital twin predicted sites, establishing them as viable targets for ablation. Table 2 shows the comparison of electrogram abnormalities identified at predicted and non-predicted sites. Figure 3 shows several examples of invasively mapped substrate, the digital twin predictions and the final ablation lesion set applied.

We then compared electrogram characteristics at other tissue regions based on accepted bipolar voltage cut-offs including the borderzone (0.5mV – 1.5mV) and healthy areas (> 1.5mV). At each region, predicted areas demonstrated increased frequency of electrogram abnormalities as well as more prolonged electrogram duration compared to voltage-matched, non-predicted areas, as shown in Figure 4. Figure S4 shows a comparison of EGM duration and abnormalities between predicted and non-predicted sites for each of the 18 cases in the study.

Comparison of substrate abnormalities at primary versus secondary predicted sites

To compare the differences between electrograms at digital twin-predicted primary and secondary sites, we undertook a sub-analysis of the substrate at each site. The mean number of predicted sites was 5.3 (± 1.8) per patient comprising on average 3.5 (± 1.2) primary sites and 1.8 (± 1.3) secondary sites. Mean predicted area was 10.9 cm^2 (± 3.9 cm^2) which constituted 22.2% (18.2 – 34.6%) of the total scar area. Predicted site area was comprised of 7.7 cm^2 (± 2.6 cm^2) from primary sites and 3.2 cm^2 (± 3.2 cm^2) from secondary sites. 6/18 (33.3%) of patients had no secondary predicted sites in the digital twins.

Within areas of low voltage (< 1.5mV), double potentials, late potentials and other LAVA were more frequent in primary compared to secondary sites, however prevalence of all electrogram abnormalities combined did not significantly differ between primary and secondary sites, being present in 710/1748 (40.6%) of primary sites vs 406/1074 (37.8%) of secondary sites (p = 0.14). There were no significant differences in measures of electrogram timing between primary and secondary sites, with an overall electrogram duration of 77.9ms (± 26.6ms) at primary sites compared to 76.9ms (± 24.4ms) at secondary sites (p = 0.30). These differences are summarised in Table 3 and indicate that from a substrate perspective, primary sites do not differ significantly from secondary sites.

Evaluation of functional substrate mapping at digital twin predicted sites

We next assessed the electrophysiological parameters of predicted sites using two forms of functional substrate mapping: extrastimulus mapping to detect electrogram prolongation under stress and slow conducting regions, as evidenced by deceleration zones on ILAM. 6866 bipolar extrastimulus electrograms were analysed. Abnormalities were observed in 1312/2773 (47.3%) of predicted site electrograms compared to 1116/4093 (27.3%) of non-predicted site electrograms (p < 0.001). Mean electrogram duration remained longer at predicted sites compared to non-predicted sites (87.7ms [± 31.3ms] vs 73.9ms [± 23.7ms], p < 0.001) and the average electrogram prolongation in response to extrastimulus pacing was greater at predicted sites compared to non-predicted sites (11.7ms [± 16.5ms] vs 7.5ms [± 8.5ms], p = 0.02). These results indicate that the heart digital twin's prediction sites respond particularly poorly to conditions of stress, which is a hallmark of the critical VT isthmus.

On ILAM mapping, a total of 26 deceleration zones were identified, indicating regions of conduction slowing. There was a mean of 1.44 (± 1.20) DZ per patient. 23/26 (88.5%) were located on the endocardium, with 3/26 (11.5%) located on the epicardium. 21/26 (80.8%) of RV paced DZ were located within 5mm of a predicted site. The median geodesic distance from the center of the DZ to the closest predicted area was 1mm (range 0 – 32mm). 18 out of the 26 (69.2%) DZ were located closest

to a primary predicted site whereas 8/26 (30.8%) were located closest to a secondary predicted site. These results suggest that the digital twin predictions accurately detect regions of slow conduction, which are essential for the formation of re-entry. Figure 5 shows a patient with ICM and lateral wall scar where isochronal late activation mapping revealed a deceleration zone along the anterior edge of the low-voltage area. This corresponded to a predicted site from the patient's digital twin.

VT induction and entrainment mapping

Following substrate mapping, monomorphic VT was inducible in 15/18 (83.3%) patients. 2/18 (11.1%) were not inducible to any ventricular arrythmia, whilst 1/18 (5.6%) was only inducible for VF. Due to haemodynamic instability in most patients, entrainment mapping was only possible in 4/18 (22.2%) cases. In 3 out of the 4 patients (75.0%), mid-diastolic activity during VT and entrainment with concealed fusion was found within 5mm of a predicted site.

Discussion

This study presents the first combined prospective heart digital twin and clinical study in which patients requiring VT ablation not only undergo personalized arrhythmia simulation and prediction of optimum ablation lesions but also systematic analysis of the invasive electrophysiological substrate. This approach allowed for a comprehensive validation of the heart digital twins by identifying the characteristics of the prediction in relation to the substrate abnormalities and comparing them to bystander regions within the scar, demonstrating significant differences between the predicted and bystander regions. This study is crucial in demonstrating to electrophysiologists the emerging role of modeling-guided VT ablation and therefore serves as a bridge to bringing the routine use of heart digital twins in guiding VT ablation closer to reality.

Prediction of substrate abnormalities

The main findings of this study are that digital twins' predictions of the critical targets for VT ablation exhibit greater electrogram abnormalities during substrate mapping compared to voltage-matched, non-predicted areas. Furthermore, electrogram behaviour in response to stress during functional substrate mapping was particularly abnormal at predicted sites compared to non-predicted sites and areas of conduction slowing, which are crucial for the establishment of re-entry, frequently arose at these predicted sites. In a departure from other digital twin development studies, we include patients with both NICM as well as ICM to show that this technology can be utilized regardless of etiology to detect arrhythmogenic sites.

Substrate-based VT ablation relies on the identification of abnormal electrograms as a surrogate for the VT isthmus. Predicted sites from digital twins exhibited 41% greater frequency of electrogram abnormalities compared to non-predicted sites, therefore establishing their utility in guiding VT ablation. These abnormalities represent valid targets for substrate-based ablation and have been

shown to correlate closely with the VT isthmus.[38] Furthermore, electrogram duration was also prolonged at predicted sites compared to non-predicted sites. EGM duration is known to predict the VT isthmus, with termination of the VT frequently achieved when the longest duration electrograms are targeted.[39] The finding that a high proportion of deceleration zones co-locate to these predicted areas also underscores that the digital twin technology is capable of accurately detecting conduction slowing and isochronal crowding, which has emerged as a valid and effective approach to control VT.[40,41]

EAM low voltage vs MRI scar – which is the gold standard?

Substrate-based VT ablation relies on accurate detection of myocardial scar followed by either complete scar homogenisation or elimination of the abnormal electrograms within the scar.[7,42] Similarly, for heart digital twins to be effective, tissue characterisation based on MRI signal intensity must accurately reflect the presence or absence of fibrotic tissue in the substrate. In our study, we showed a discrepancy in size between bipolar endocardial voltage defined scar using conventional cut-off values and the MRI-derived scar, with the bipolar EAM underestimating the size of the scar. By contrast, the unipolar voltage map correlated more closely with the MRI-defined scar. Reasons for this include the inability of bipolar mapping techniques to 'visualise' epicardial or mid-myocardial scar. Furthermore, traditional cut-off values of 1.5mV bipolar voltage were derived from a low number of patients, confined to the ICM population, using the larger electrodes of ablation catheters to acquire the data.[43,44] Another variable in MRI scar estimation is the variation in signal thresholding values that can be used during the creation of the digital twin. Importantly, we show that despite being labelled as "healthy" by bipolar voltage (>1.5mV), there are still abnormalities in nearly 5% of electrograms. This was particularly true when the electrogram was located within areas of MRI-defined scar. Therefore, it is highly likely that a personalized voltage cut-off is required to define scar rather than a blanket value for all patients and all aetiologies.

The relative importance of primary vs secondary sites in predicting substrate abnormalities

Over one third of patients undergoing VT ablation will require a repeat procedure at some stage.[45] Redo VT ablation is characterised by longer duration, greater technical difficulty and higher complication rates compared to first time ablation.[45,46] Heart digital twins have the unique advantage in predicting not only locations of critical importance to the VT circuit in the native scar substrate, but also emergent locations in the new "landscape" (including scar plus lesions), and may therefore reduce the requirement for redo VT ablation. Our study is the first to compare the substrate characteristics between digital twin sites identified in the initial substrate and those identified following the application of a primary ablation lesion set. Overall prevalence of electrogram abnormalities and total electrogram duration were similar between primary and secondary sites and we postulate that the relatively small difference is seen because both sites are able to sustain VT under the right circumstances. Substrate abnormalities are arrhythmogenic, but not sufficient in isolation for VT to occur. Functional components and stochastic events such as premature ventricular complexes are required to initiate and sustain a VT circuit. The identified secondary VTs require that a new area of block, generated by the primary ablation lesions, is present before a subsequent VT can occur. However, they still require the correct electrophysiological milieu to sustain a re-entrant circuit.

Implications for the use of digital twins in guiding VT ablation

Heart digital twin technology takes advantage of a readily available pre-procedural imaging modality to non-invasively predict the likely locations of a patient's VT. Furthermore, it has the potential to determine the most efficient ablation strategy that will terminate all potential VT circuits a patient may harbour and can be used to help guide the need for epicardial access during VT ablation. By accurately predicting regions enriched with substrate abnormalities, a digital twin-guided substrate ablation may help avoid the requirement for VT induction and mapping, which can be time-consuming and lead to haemodynamic instability. Furthermore, digital twins may allow an ablation strategy directly guided by the digital twin, without the need for comprehensive substrate mapping. Having a model pre-

procedurally that provides guidance to the operator on where to focus on to achieve rapid control of most re-entrant circuits would lead to more manageable procedures with lower overall risk and duration. Furthermore, the total ablation area predicted by the digital twin is significantly smaller than the EAM or MRI detected scar area, implying that a digital twin-guided ablation would potentially result in a lower burden of ablation, again reducing procedural time and complication risk. Due to the iterative nature of the modeling process, whereby simulations are repeated following application of the first set of ablation lesions to assess for the emergence of secondary VTs, this technology could also help reduce the requirement for repeat ablation, which are performed in an unacceptably high proportion of VT patients.

Limitations

The heart digital twins described in this study are computationally expensive, requiring high-performance infrastructure and hours of simulation runs. However, efforts are underway to use AI and other techniques to brings simulation times down to minutes or even seconds, thus rendering the technology scalable so it can be used across centers. Accuracy of the models is dependent on obtaining high quality LGE-CMR images, which can be challenging in the clinical environment and is particularly prone to artefact in patients with ICDs, as demonstrated by the final recruitment rate of only 50% of screened patients. This issue is expected to be improved with more prevalent adoption of wideband imaging techniques as well as the integration of AI in image segmentation. Our experience was that as familiarity with the 3D LGE-CMR sequence improved throughout the study, the rates of acquiring adequate image quality improved significantly over time. Digital twin predictions also require validation in prospective studies of VT mapping and induction, which remain the current gold-standard for VT ablation. These studies are in progress. Coregistration of the EAM with the MRI model was not automated and relied on expert approximation of the two surfaces. Small mismatches in surface co-registration could result in large discrepancies in the labelling of predicted and non-predicted sites. Digital twin ablation lesions are assumed to be transmural with a uniform radius of 3.5mm. This

consistency is unlikely to be achieved clinically and transmurality is far from guaranteed, particularly in thick-walled structures such as the interventricular septum or LV summit.

In conclusion, we present the first combined personalized computational and invasive electrophysiological study to validate the use of heart digital twins in predicting critical substrate abnormalities in scar-dependent VT. Digital twins represent a potential paradigm shift towards the application of personalized medicine in the treatment of arrhythmia. This study demonstrates their utility and accuracy in predicting the conventional invasive abnormalities targeted by modern substrate-based VT ablation. We expect these findings will serve to increase the trust clinicians place in this innovative technology and propel the mainstream use of digital twin-guided VT ablation.

Ethical approval

All patients described in this study provided written, informed consent. The study was approved by Health Research Authority (HRA) London – Surrey Research Ethics Committee (21/LO/0083). Clinicaltrials.gov reference number: NCT04632394.

Funding sources

MW has received funding through the Advanced Ventricular Arrhythmia Training and Research Project, administered by the St George's Hospital Charity (RES 20 21 001). NT has received grant funding from the National Institutes of Health (R01HL142496 and R01HL166759) and a grant from the Leducq Foundation. MS and AL have received modest, restricted grants from Abbott Laboratories.

Conflicts of interest disclosures

None.

Supplemental Material

Supplemental Methods

Supplemental Tables S1-3

Supplemental Figures S1-4

References 47-52

References

1. Sapp JL, Wells GA, Parkash R, et al.: Ventricular Tachycardia Ablation versus Escalation of Antiarrhythmic Drugs. *N Engl J Med*. 2016; 375:111–121.

2. Reddy VY, Reynolds MR, Neuzil P, et al.: Prophylactic Catheter Ablation for the Prevention of Defibrillator Therapy. *N Engl J Med*. 2007; 357:2657.

3. Kuck K-H, Schaumann A, Eckardt L, et al.: Catheter ablation of stable ventricular tachycardia before defibrillator implantation in patients with coronary heart disease (VTACH): a multicentre randomised controlled trial. *Lancet*. 2010; 375:31–40.

4. Stevenson WG, Khan H, Sager P, et al.: Identification of reentry circuit sites during catheter mapping and radiofrequency ablation of ventricular tachycardia late after myocardial infarction. *Circulation*. 1993; 88:1647–1670.

5. Stevenson WG, Delacretaz E, Friedman PL, Ellison KE: Identification and ablation of macroreentrant ventricular tachycardia with the CARTO electroanatomical mapping system. *PACE*. 1998; 21:1448–1456.

6. Nakahara S, Tung R, Ramirez RJ, et al.: Distribution of late potentials within infarct scars assessed by ultra high-density mapping. *Heart Rhythm.* 2010; 7:1817–1824.

7. Jaïs P, Maury P, Khairy P, et al.: Elimination of local abnormal ventricular activities: a new end point for substrate modification in patients with scar-related ventricular tachycardia. *Circulation.* 2012; 125:2184–2196.

8. Di Biase L, Santangeli P, Burkhardt DJ, et al.: Endo-epicardial homogenization of the scar versus limited substrate ablation for the treatment of electrical storms in patients with ischemic cardiomyopathy. *J Am Coll Cardiol*. 2012; 60:132–141.

9. Kuck KH, Tilz RR, Deneke T, et al.: Impact of substrate modification by catheter ablation on implantable cardioverter-defibrillator interventions in patients with unstable ventricular arrhythmias and coronary artery disease: Results from the multicenter randomized controlled SMS (Substrate Modification Study). *Circ Arrhythm Electrophysiol*. 2017; 10:e004422.

10. Tung R, Xue Y, Chen M, et al.: First-Line Catheter Ablation of Monomorphic Ventricular Tachycardia in Cardiomyopathy Concurrent With Defibrillator Implantation: The PAUSE-SCD Randomized Trial. *Circulation*. 2022; 145:1839–1849.

11. Della Bella P, Baratto F, Vergara P, et al.: Does Timing of Ventricular Tachycardia Ablation Affect Prognosis in Patients With an Implantable Cardioverter Defibrillator? Results From the Multicenter Randomized PARTITA Trial. *Circulation*. 2022; 145:1829–1838.

12. Willems S, Tilz RR, Steven D, et al.: Preventive or Deferred Ablation of Ventricular Tachycardia in Patients With Ischemic Cardiomyopathy and Implantable Defibrillator (BERLIN VT). *Circulation*. 2020; 141:1057–1067.

13. Ding WY, Pearman CM, Bonnett L, et al.: Complication rates following ventricular tachycardia ablation in ischaemic and non-ischaemic cardiomyopathies: a systematic review. *JICE*. 2022; 63:59–67.

14. Tung R, Boyle NG, Shivkumar K: Catheter Ablation of Ventricular Tachycardia. *Circulation*. 2010; 122:389-391.

15. National Academies of Sciences Egineering and Medicine: Foundational Research Gaps and Future Directions for Digital Twins. Foundational Research Gaps and Future Directions for Digital Twins, 2024, available from: https://www.ncbi.nlm.nih.gov/books/NBK605507/

16. Laubenbacher R, Mehrad B, Shmulevich I, Trayanova N: Digital Twins in Medicine. *Nat Comput Sci.* 2024; 4:184–191.

17. Trayanova N, Prakosa A, Up digital and personal: How Heart Digital Twins can Transform Patient Care. *Heart Rhythm*. 2024, 21:89-99.

18. Shade JK, Prakosa A, Popescu DM, et al.: Predicting risk of sudden cardiac death in patients with cardiac sarcoidosis using multimodality imaging and personalized heart modeling in a multivariable classifier. *Science Advances*. 2021; 7:8020–8048.

19. O'hara RP, Binka E, Prakosa A, et al.: Personalized computational heart models with T1-mapped fibrotic remodeling predict sudden death risk in patients with hypertrophic cardiomyopathy. *eLife*. 2022; 11:e73325.

20. Arevalo HJ, Vadakkumpadan F, Guallar E, et al.: Arrhythmia risk stratification of patients after myocardial infarction using personalized heart models. *Nat Commun*. 2016; 7, 11437.

21. Zhang Y, Zhang K, Prakosa A, et al.: Predicting Ventricular Tachycardia Circuits in Patients with Arrhythmogenic Right Ventricular Cardiomyopathy using Genotype-specific Heart Digital Twins. *eLife*. 2023; 12:RP88865.

22. Sung E, Prakosa A, Zhou S, et al.: Fat infiltration in the infarcted heart as a paradigm for ventricular arrhythmias. *Nat Cardiovasc Res*. 2022; 1:933–945.

23. Sung E, Prakosa A, Aronis KN, et al.: Personalized Digital-Heart Technology for Ventricular Tachycardia Ablation Targeting in Hearts With Infiltrating Adiposity. *Circ Arrhythm Electrophysiol*. 2020; 13:E008912.

24. Prakosa A, Arevalo HJ, Deng D, et al.: Personalized virtual-heart technology for guiding the ablation of infarct-related ventricular tachycardia. *Nat Biomed Eng*. 2018; 2:732–740.

25. Shade JK, Cartoski MJ, Nikolov P, et al.: Ventricular arrhythmia risk prediction in repaired Tetralogy of Fallot using personalized computational cardiac models. *Heart Rhythm*. 2020; 17:408–414.

26. Prakosa A, Malamas P, Zhang S, et al.: Methodology for image-based reconstruction of ventricular geometry for patient-specific modeling of cardiac electrophysiology. *Prog Biophys Mol Biol*. 2014; 115:226–234.

27. Schmidt A, Azevedo CF, Cheng A, et al.: Infarct Tissue Heterogeneity by Magnetic Resonance Imaging Identifies Enhanced Cardiac Arrhythmia Susceptibility in Patients With Left Ventricular Dysfunction. *Circulation*. 2007; 115:2006–2014.

28. Boyle PM, Ochs AR, Ali RL, Paliwal N, Trayanova NA: Characterizing the arrhythmogenic substrate in personalized models of atrial fibrillation: sensitivity to mesh resolution and pacing protocol in AF models. *Europace.* 2021; 23:I3–I11.

29. Bayer JD, Blake RC, Plank G, Trayanova NA: A novel rule-based algorithm for assigning myocardial fiber orientation to computational heart models. *ABME*. 2012; 40:2243–2254.

30. Ten Tusscher KHWJ, Noble D, Noble PJ, Panfilov A V.: A model for human ventricular tissue. *Am J Physiol Heart Circ Physiol*. 2004; 286:1573–1589.

31. Plank G, Loewe A, Neic A, et al.: The openCARP simulation environment for cardiac electrophysiology. *Comput Methods Programs Biomed*. 2021; 208:106223.

32. Battaglia A, Odille F, Magnin-Poull I, et al.: An efficient algorithm based on electrograms characteristics to identify ventricular tachycardia isthmus entrance in post-infarct patients. *Europace*. 2020; 22:109–116.

33. Chillou C De, Magnin-Poull I, Andronache M, et al.: Showing up channels for postinfarct ventricular tachycardia ablation. *PACE*. 2012; 35:897–904.

34. Irie T, Yu R, Bradfield JS, et al.: Relationship between sinus rhythm late activation zones and critical sites for scar-related ventricular tachycardia. *Circ Arrhythm Electrophysiol*. 2015; 8:390–399.

35. Aziz Z, Shatz D, Raiman M, et al.: Targeted Ablation of Ventricular Tachycardia Guided by Wavefront Discontinuities during Sinus Rhythm: A New Functional Substrate Mapping Strategy. *Circulation*. 2019; 140:1383–1397.

36. Roca-Luque I, Zaraket F, Garre P, et al.: Accuracy of standard bipolar amplitude voltage thresholds to identify late potential channels in ventricular tachycardia ablation. *JICE*. 2023; 66:15.

37. Hutchinson MD, Gerstenfeld EP, Desjardins B, et al.: Endocardial Unipolar Voltage Mapping to Detect Epicardial Ventricular Tachycardia Substrate in Patients With Nonischemic Left Ventricular Cardiomyopathy. *Circ Arrhythm Electrophysiol*. 2011; 4:49–55.

38. Zachariah D, Nakajima K, Rosario Limite L, et al.: Significance of abnormal and late ventricular signals in ventricular tachycardia ablation of ischemic and nonischemic cardiomyopathies. *Heart Rhythm*. 2022; 19:2075-2083.

39. Rossi P, Cauti FM, Niscola M, et al.: Ventricular Electrograms Duration Map to Detect Ventricular Arrhythmia Substrate: the VEDUM Project Study. *Circ Arrhythm Electrophysiol*. 2023; 16:447–455.

40. von Alvensleben JC, Sandhu A, Nash D, et al.: MP-453092-5 Isochronal Late Activation Mapping for Targeted Ablation of Ventricular Tachycardia in Patients with Tetralogy of Fallot. *Heart Rhythm*. 2023; 20:S130–S131.

41. Uotani Y, Okubo Y, Komatsu Y, Nogami A, Aonuma K, Nakano Y: Isochronal late activation mapping of epicardial ventricular tachycardia in a patient with midventricular obstructive hypertrophic cardiomyopathy. *HRCR*. 2022; 8:374–377.

42. Gökoğlan Y, Mohanty S, Gianni C, et al.: Scar Homogenization Versus Limited-Substrate Ablation in Patients With Nonischemic Cardiomyopathy and Ventricular Tachycardia. *J Am Coll Cardiol*. 2016; 68:1990–1998.

43. Reddy VY, Wrobleski D, Houghtaling C, Josephson ME, Ruskin JN: Combined epicardial and endocardial electroanatomic mapping in a porcine model of healed myocardial infarction. *Circulation*. 2003; 107:3236–3242.

44. Tschabrunn CM, Roujol S, Dorman NC, Nezafat R, Josephson ME, Anter E: High-Resolution Mapping of Ventricular Scar: Comparison Between Single and Multielectrode Catheters. *Circ Arrhythm Electrophysiol*. 2016; 9:e003843.

45. Tzou WS, Tung R, Frankel DS, et al.: Outcomes after repeat ablation of ventricular tachycardia in structural heart disease: An analysis from the International VT Ablation Center Collaborative Group. *Heart Rhythm*. 2017; 14:991–997.

46. Garcia Garcia J, Arya A, Dinov B, et al.: Impact of repeat ablation of ventricular tachycardia in patients with structural heart disease. *Europace*. 2024; 26:1-10.

47. Toussaint N, Mansi T, Delingette H, Ayache N, Sermesant M: An integrated platform for dynamic cardiac simulation and image processing: Application to personalised tetralogy of fallot simulation. *EG VCBM 2008 - Eurographics Workshop on Visual Computing for Biomedicine*. 2008; 21–28.

48. Bayer JD, Beaumont J, Krol A: Laplace–Dirichlet Energy Field Specification for Deformable Models. An FEM Approach to Active Contour Fitting. *ABME*. 2005; 33:1175–1186.

49. Weiss DL, Seemann G, Keller DUJ, Farina D, Sachse FB, Dössel O: Modeling of heterogeneous electrophysiology in the human heart with respect to ECG genesis. *Comput Cardiol*. 2007, 49–52.

50. Yao JA, Hussain W, Patel P, Peters NS, Boyden PA, Wit AL: Remodeling of gap junctional channel function in epicardial border zone of healing canine infarcts. *Circ Res*. 2003; 92:437–443.

51. Plank G, Zhou L, Greenstein JL, et al.: From mitochondrial ion channels to arrhythmias in the heart: Computational techniques to bridge the spatio-temporal scales. *Phil Trans R Soc*. 2008; 366:3381–3409.

52. Bishop MJ, Rodriguez B, Qu F, Efimov IR, Gavaghan DJ, Trayanova NA: The Role of Photon Scattering in Optical Signal Distortion during Arrhythmia and Defibrillation. *Biophys J*. 2007; 93:3714.

Tables

Table 1: Baseline demographics of the cohort. AAD = anti-arrhythmic drug, ICD = implantable cardioverter-defibrillator, CRT-D = cardiac resynchronisation therapy – defibrillator. EAM = electroanatomical map.

	ICM (15)	**NICM (3)**	**Total (18)**
Age (years)	67.7 (± 9.7)	71.7 (± 7.4)	68.4 (± 9.5)
Male sex	14 (93.3%)	3 (100%)	17 (94.4%)
Baseline EF (%)	41.5 (± 17.7)	46.3 (± 10.0)	42.3 (± 16.5)
NYHA class			
I	7 (46.6%)	1(33.3%)	8 (44.4%)
II	5 (33.3%)	2 (66.7%)	7 (38.9%)
III	3 (20.0%)	0	3 (16.7%)
IV	0	0	0
Hypertension	11 (73.3%)	2 (66.7%)	13 (72.2%)
Diabetes	6 (40.0%)	1 (33.3%)	7 (38.9%)
Atrial fibrillation	6 (40.0%)	2 (66.7%)	8 (44.4%)
Chronic kidney disease	7 (46.7%)	2 (66.7%)	9 (50.0%)
Beta-blocker	14 (93.3%)	3 (100%)	17 (94.4%)
Amiodarone	4 (26.7%)	3 (100%)	7 (38.9%)
Mexiletine	2 (13.3%)	1 (33.3%)	3 (16.7%)
ICD	12 (80.0%)	3 (100%)	15 (83.3%)
CRT-D	2 (10.7%)	0	2 (11.1%)
Prior VT ablation	2 (13.3%)	0	2 (11.1%)
Prior cardiac surgery	6 (40.0%)	0	6 (33.3%)
Epicardial mapping	3 (16.7%)	2 (66.7%)	5 (27.8%)

Table 2: Comparison of bipolar voltage and electrogram characteristics from within areas of dense scar according to accepted cut-offs (bipolar voltage <0.5mV) between predicted and non-predicted sites. EGM = electrogram, LAVA = local abnormal ventricular activity.

Parameter	**Predicted (n = 1029)**	**Non-predicted (n = 1611)**	**P - value**
Voltage			
Bipolar voltage (mV)	0.31 (± 0.11)	0.32 (± 0.11)	0.69
Electrogram characteristics			
Fractionation	408/1029 (39.7%)	435/1611 (27.0%)	< 0.001
Double potential	25/1029 (2.4%)	24/1611 (1.5%)	0.08
Late potential	40/1029 (3.9%)	18/1611 (1.1%)	< 0.001
Other LAVA	86/1029 (8.4%)	90/1611 (5.6%)	0.01
Any EGM abnormality	468/1029 (45.5%)	519/1611 (32.2%)	< 0.001
Electrogram timing			
EGM onset (ms)	50.8 (± 31.9)	57.9 (± 31.7)	< 0.001
EGM offset (ms)	132.8 (± 26.9)	127.5 (± 25.0)	< 0.001
EGM duration (ms)	82.0 (± 25.9)	69.7 (± 22.3)	< 0.001
EGM offset to QRS offset (ms)	33.1 (± 28.0)	36.1 (± 27.8)	0.01

Table 3: Comparison of primary vs secondary predicted sites within low voltage area (<1.5mV). EGM = electrogram, LAVA = local abnormal ventricular activity.

Parameter	**Primary (n = 1748)**	**Secondary (n = 1074)**	**P - value**
Voltage			
Bipolar voltage (mV)	0.72 (± 0.39)	0.71 (± 0.41)	0.26
Electrogram characteristics			
Fractionation	573/1748 (32.8%)	118/1074 (32.8%)	1.0
Double potential	75/1748 (4.3%)	23/1074 (2.1%)	0.002
Late potential	103/1748 (5.9%)	26/1074 (2.4%)	< 0.001
Other LAVA	178/1748 (10.2%)	67/1074 (6.2%)	< 0.001
Any EGM abnormality	710/1748 (40.6%)	406/1074 (37.8%)	0.14
Electrogram timing			
EGM onset (ms)	55.0 (± 28.2)	55.5 (± 30.3)	0.66
EGM offset (ms)	132.9 (± 28.9)	132.3 (± 27.1)	0.33
EGM duration (ms)	77.9 (± 26.6)	76.9 (± 24.4)	0.30
EGM offset to QRS offset (ms)	35.3 (± 30.6)	34.1 (± 28.5)	0.30

Figures

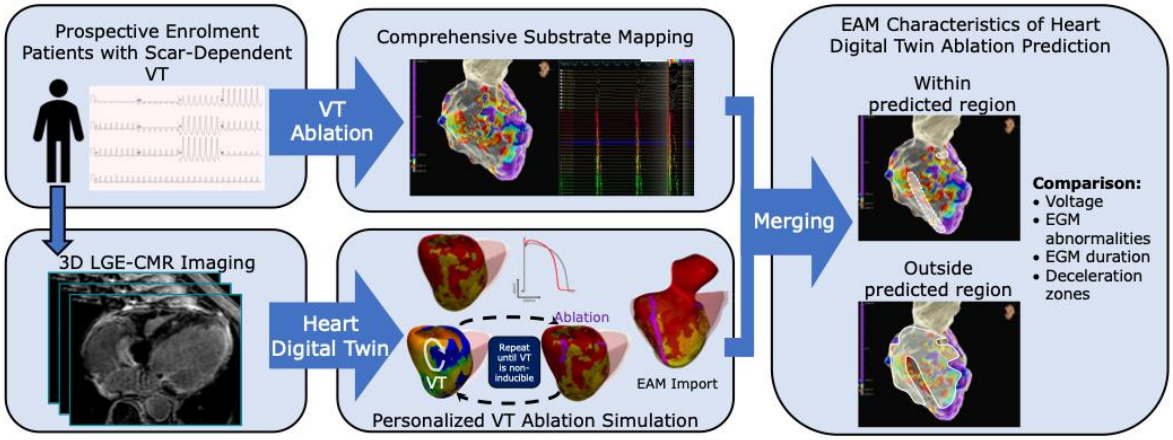

Figure 1: Study overview. Prospective scar-dependent VT patients were recruited and underwent high quality 3D LGE-CMR (left). Patients underwent personalized cardiac digital twin creation (middle, bottom) with iterative VT induction and ablation to reveal and terminate all VTs including post-ablation emergent arrhythmias. Patients also underwent comprehensive substrate mapping (middle, top) and invasive VT ablation. Digital twin predictions were merged with the substrate map for comparison of substrate abnormalities digital twin-predicted sites and sites outside the predicted regions (right). EGM – electrogram.

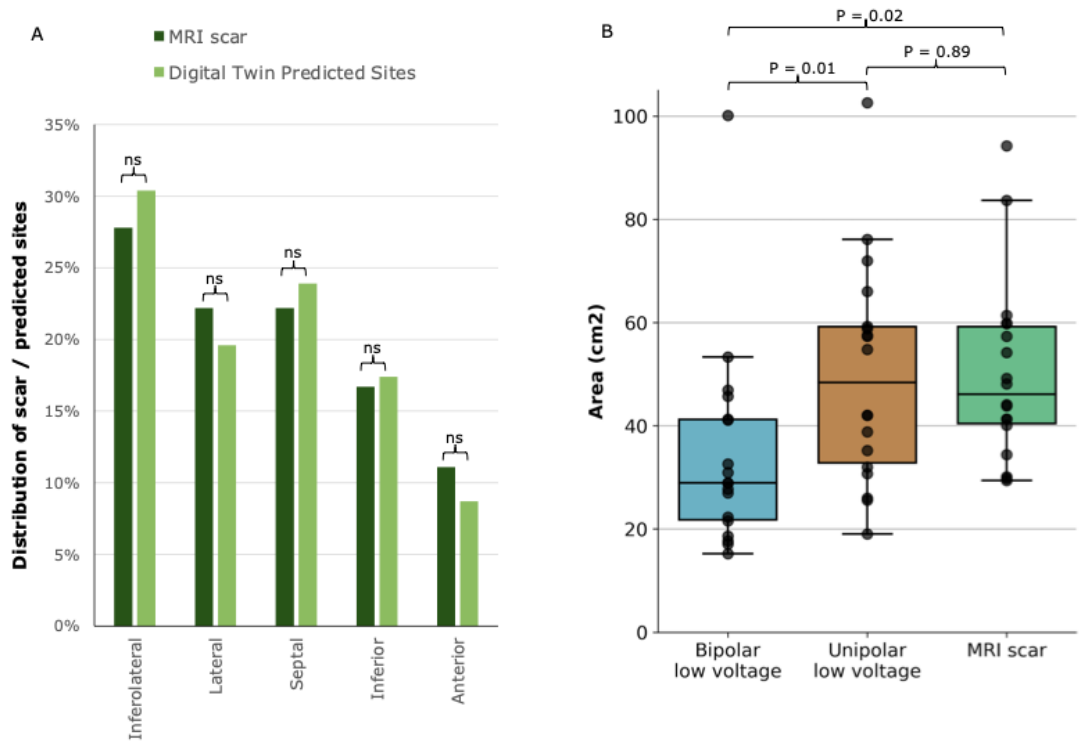

Figure 2: A - Predominant left ventricular scar location and digital twin-predicted site location within the cohort. B – Comparison of bipolar low voltage area, unipolar low voltage area and MRI-defined scar area.

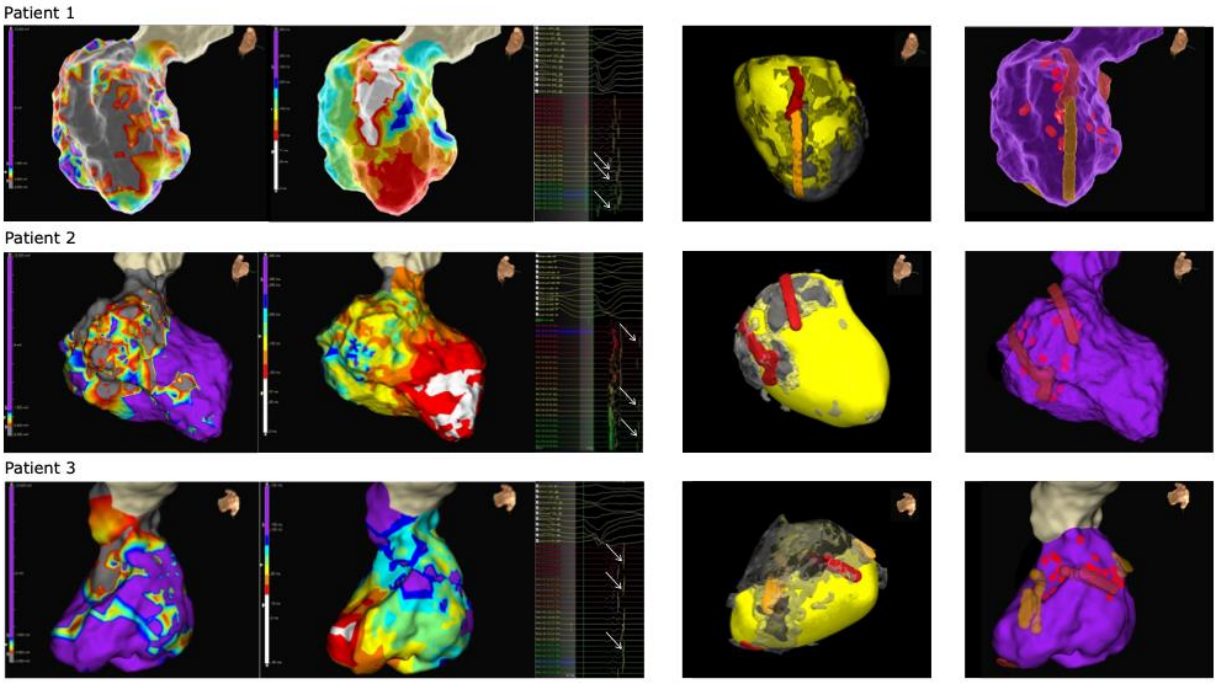

Figure 3**:** Representative examples of three patients who underwent invasive substrate mapping (left column) including voltage and activation mapping, with example abnormal EGMs displaying fractionation and late potentials (white arrows). Middle column shows the digital twin model with MRI infarct (grey) and predicted sites (primary in red, secondary in orange). Right column shows final ablation lesion (red circles) set in comparison to the predicted sites.

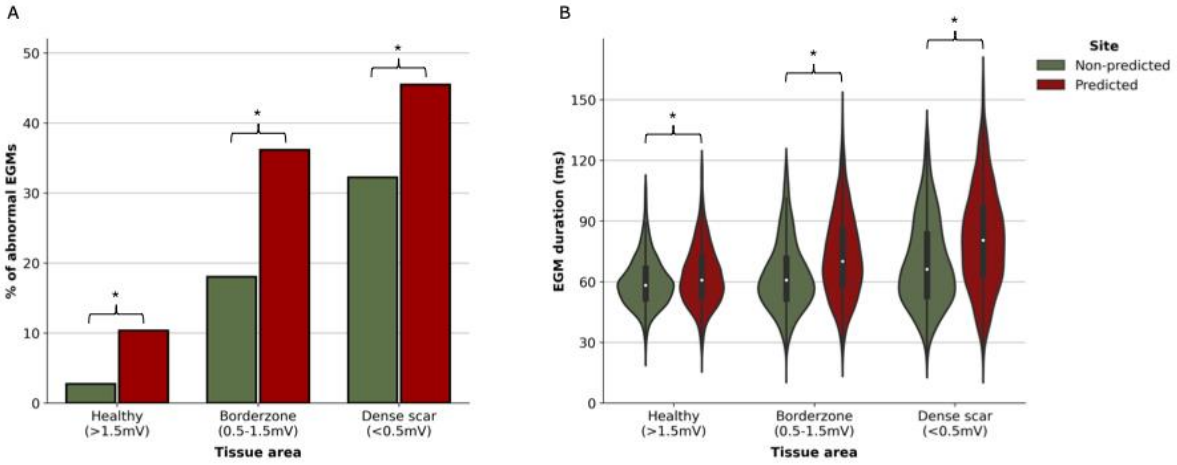

Figure 4: Comparison of prevalence of electrogram abnormalities (A) and electrogram duration (B) between predicted and non-predicted sites, stratified by tissue region. * denotes statistical significance. EGM – electrogram.

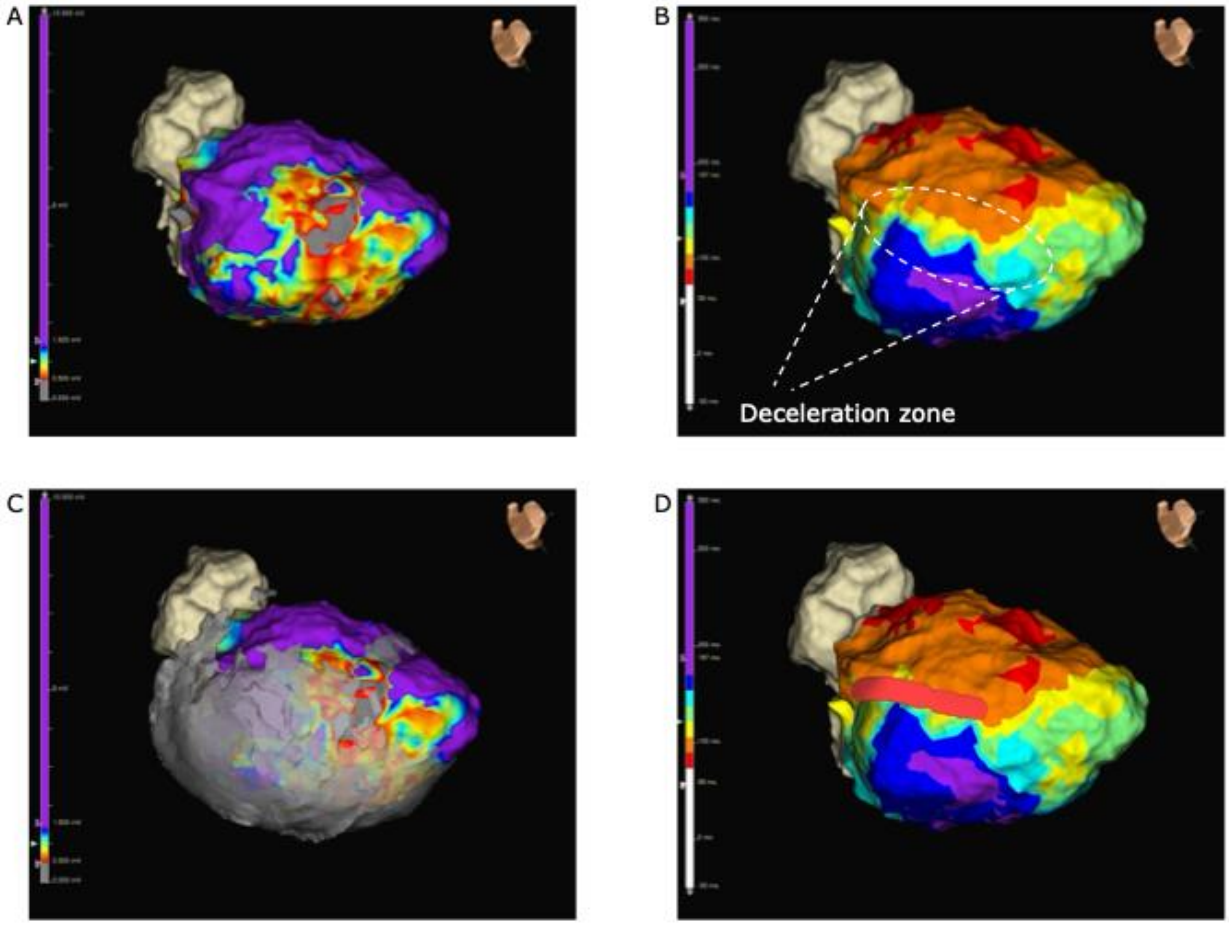

Figure 5: Example of conduction slowing correctly predicted by the patient's digital twin. A – substrate mapping revealed inferolateral wall scar. B – isochronal late activation mapping demonstrating a deceleration zone (white oval). C – Voltage map with MRI scar overlaid. D – deceleration zone corresponds to a digital twin predicted site on inferoseptal border of scar.